

Molecular-beam epitaxy of (Zn,Mn)Se on Si(100)

T. Slobodskyy, C. Rüster, R. Fiederling, D. Keller, C. Gould, W. Ossau, G. Schmidt, and L. W. Molenkamp
Physikalisches Institut, Universität Würzburg, Am Hubland, 97074 Würzburg, Germany

(Dated: November 21, 2018)

We have investigated the growth by molecular-beam epitaxy of the II-VI diluted magnetic semiconductor (Zn,Mn)Se on As-passivated Si(100) substrates. The growth start has been optimized by using low-temperature epitaxy. Surface properties were assessed by Nomarski and scanning electron microscopy. Optical properties of (Zn,Mn)Se have been studied by photoluminescence and a giant Zeeman splitting of up to 30 meV has been observed. Our observations indicate a high crystalline quality of the epitaxial films.

The availability of the proper material systems for spin injection, manipulation, and detection will play an important role in further progress in the field of spintronics.

II-VI diluted magnetic semiconductors (DMS) are known[1] to be good candidates for effective spin injection into a nonmagnetic semiconductor (NMS) because their spin polarization is nearly 100% and their conductivity is comparable to that of typical NMS. Moreover, II-VI DMSs can be n-type doped, thus avoiding the very fast spin precession that limits the applicability of ferromagnetic III-V DMSs as spin injector.

A very promising II-VI DMS for spin injection is (Zn,Mn)Se, which has been previously used for spin injection experiments into GaAs[2], and ZnSe[3].

However, these compound semiconductors are by no means the optimal NMS materials for spin injection experiments because of their limited spin lifetime. Silicon, because of its higher crystalline symmetry, has a very long spin-flip length[4]. Moreover, it is evidently in standard use in the semiconductor industry and therefore a very attractive material for future spintronic devices.

It therefore seems natural to attempt spin injection from (Zn,Mn)Se into Si. However, the surface reactivity of Si and the lattice mismatch between Si and (Zn,Mn)Se present difficulties that require more detailed investigation. In this paper, we address the molecular-beam epitaxy (MBE) growth of (Zn,Mn)Se on Si and will demonstrate that careful optimization results in high quality epilayers.

Early experiments on the growth of the parent compound ZnSe on Si were reported in Ref.[5], where using As passivation, interfaces of reasonable quality were obtained. More recently, Chauvet et al.[6] used the lattice match between Si and the $\text{Zn}_{0.55}\text{Be}_{0.45}\text{Se}$ ternary alloy, in combination with migration enhanced epitaxy (MEE) to obtain high quality epitaxial films. Unfortunately, (Be,Zn)Se ternary alloys with a high Be concentration cannot be doped, making this approach unsuitable for the growth of structures aiming at spin injection experiments. We therefore have to resort to the growth of large-mismatch epilayers.

In order to prepare a suitable Si surface for further heteroepitaxy, we have tried several different techniques. The most suitable for our MBE system is a modified RCA cleaning procedure[7] with subsequent hydrogen passivation.

We have found that hydrogen passivation thus obtained is stable in air for at least 30 minutes. During this time, the wafers are mounted on molybdenum blocks and transferred into the ultrahigh vacuum (UHV) MBE system. Indium is used as an adhesive to mount the substrates on the molybdenum blocks by heating it to temperatures of about 210 °C, which is below the hydrogen desorption temperature.

The layers are deposited in a multichamber MBE system allowing UHV transfer between the various growth chambers. Growth is performed in RIBER 2300 systems using elementary sources (6N purity). Se and As are deposited from EPI valved cracker cells and all other elements from standard effusion cells.

After degassing at 300°C for 15 min, the molybdenum blocks are transferred to the III-V growth chamber. Immediately after the transfer, the Reflection High Energy Electron Diffraction (RHEED) shows (1×1) patterns typical for hydrogen passivation. After subsequent heating of the sample to approximately 730°C, the RHEED patterns change to (1×2) , indicating desorption of the hydrogen passivation[8].

To saturate the dangling bonds and to prevent the formation of amorphous SiSe_2 [5] during (Zn,Mn)Se growth, an arsenic terminated surface is prepared by cooling the sample under arsenic flux. After this step, the Si surface is covered by a monolayer of As. Such a surface, when tilted by 4° toward (110), shows a (2×1) RHEED pattern[9]. On our exactly (100)-oriented substrates, the patterns are (2×2) , which results from a superposition of (1×2) and (2×1) patterns. This can be explained by the absence of a preferable orientation for dimer formation on an exact (100) surface[9].

After As passivation and cooling, the samples are transferred to the II-VI growth chamber where (Zn,Mn)Se films are deposited.

The growth start proves critical for successful heteroepitaxial growth of (Zn,Mn)Se on As passivated Si surfaces. The best result is obtained using a low temperature (240°C) growth start, consisting of a Zn monolayer deposition, 10 cycles of atomic layer epitaxy (ALE), 5 cycles of MEE and standard MBE of (Zn,Mn)Se at 300°C.

This procedure yields a good separation of the Si and Se layers and stimulates the relaxation of the epilayer to the lattice constant of bulk (Zn,Mn)Se. The stacking sequence of Si-Si-As-Zn-Se-Zn-Se also allows the atoms

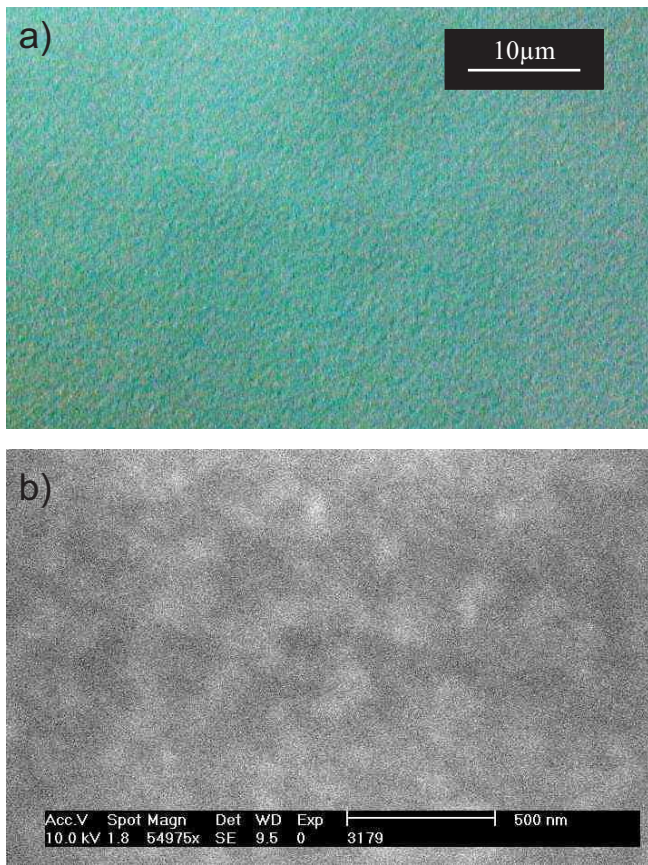


FIG. 1: (a) Polarization differential interference contrast microscopy image indicating roughness of the epitaxial surface of (Zn,Mn)Se(100) with 4% Mn surface. (b) Scanning electron microscope micrograph of the surface of a nominally identical sample.

near the interface to be fully coordinated[5].

Immediately after the start of growth, a three dimensional (3D) growth mode is observed by RHEED. This 3D growth leads to strong interactions between dislocations and usually yields an improvement in structural quality. After the ALE and MEE cycles, the growth mode stabilizes and a clear (2×1) RHEED reconstruction can be observed. During subsequent MBE, stable (2×1) RHEED patterns are observed.

Fig. 1(a) presents a polarization interference contrast microscopy image of a 200 nm thick epilayer of (Zn,Mn)Se with 4% Mn on a Si surface oriented exactly along (100). A slight surface roughness can be observed. When a nominally identical surface is viewed under higher magnification using a Scanning Electron Microscope (SEM) as in Fig. 1(b), a wavy surface structure emerges. This probably originates from the 3D growth start in combination with the lattice mismatch between the epilayer and the substrate. The mismatch leads to strain relaxation by local elastic deformation of the epilayer.

A typical High Resolution X-Ray Diffraction scan of

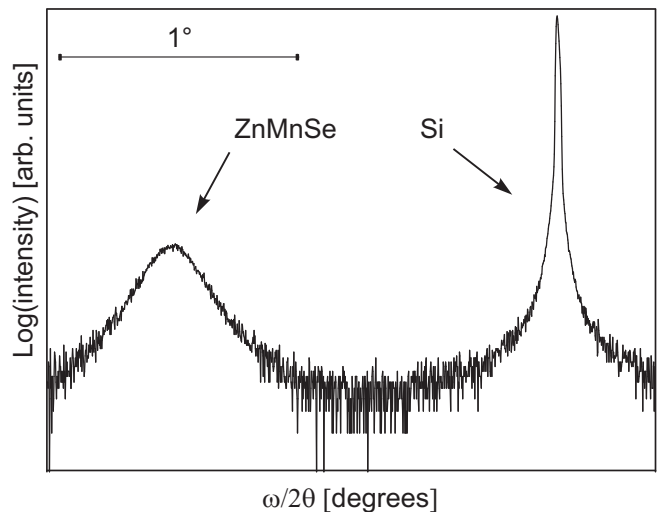


FIG. 2: $\omega/2\theta$ scan of a 200 nm (Zn,Mn)Se layer with 4% Mn taken with a (004) reflex.

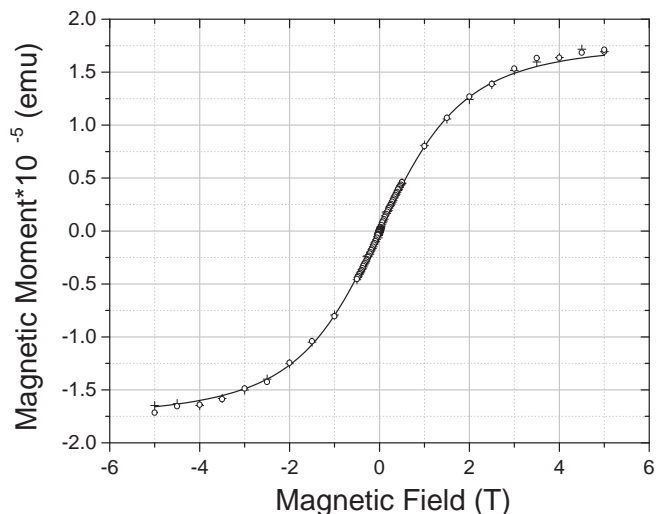


FIG. 3: Magnetic moment of a 200 nm thick (Zn,Mn)Se epilayer with 4% Mn as a function of external magnetic field as determined by SQUID magnetometry.

200 nm (Zn,Mn)Se with 4% Mn is shown in Fig. 2. The right peak corresponds to the silicon substrate and the left peak to the (Zn,Mn)Se layer. The lattice mismatch of 0.23 \AA extracted using Bragg's law from the 1.66 degree difference in peak position agrees well with the lattice mismatch expected for a fully relaxed (Zn,Mn)Se layer containing 4% Mn on Si(100). An ω scan of the (Zn,Mn)Se peak yields a Full Width at Half Maximum of about 0.4 degree, indicating an epilayer of reasonably good crystalline quality.

The magnetic properties of a 200 nm thick (Zn,Mn)Se epilayer with 4% nominal Mn concentration and volume of about $10^6 \mu\text{m}^3$ are characterized in a Quantum Design SQUID magnetometer. A 1.8 K hysteresis loop of magnetization is presented in Fig. 3. The open circles and

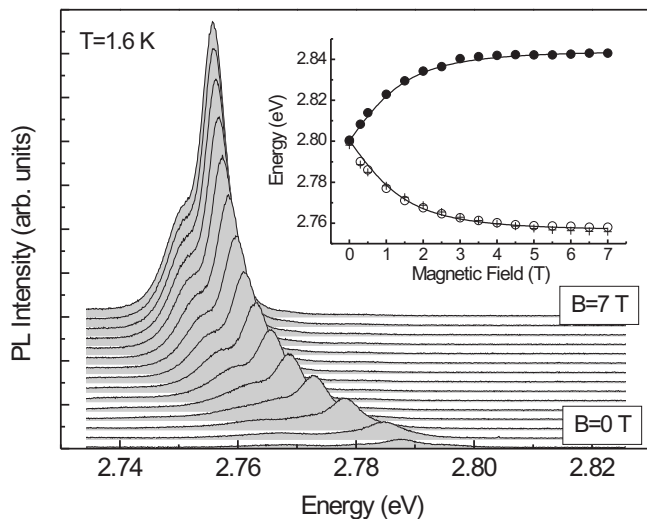


FIG. 4: Photoluminescence spectra of 1000 nm thick (Zn,Mn)Se epilayer with 2% Mn on Si(100) at various magnetic fields, detected in σ^+ - polarization. The energy dependence of the free exciton peak versus magnetic field is shown in the inset (crosses). Closed and open circles are reflectivity data for σ^+ - and σ^- - polarized light, respectively.

crosses represent the experimental data. No hysteretic behavior is observed down to the lowest resolution of the SQUID. This places an upper limit of one part per thousand for the fraction of Mn atoms with ferromagnetic behavior, and excludes the possibility that any significant portion of the Mn is present as ferromagnetic clusters.

The data is fitted well by the solid line in the figure corresponding to a modified Brillouin function[10] that is known to describe the functional dependence of the magnetization on field in (Zn,Mn)Se. This fit allows us to extract an effective temperature parameter T_e [10] of 1.45 K, which indicates[11] a Mn concentration of about 4%. The saturation magnetization is 0.2 Bohr magnetons per unit cell. Using the effective Mn spin for the interacting Mn system of (Zn,Mn)Se from Ref. [11], this corresponds to a Mn concentration of about 3.5%. Given

the fairly large uncertainty in the determination of the volume of the sample, we consider these numbers to be in fair agreement. The magnetic data is therefore entirely consistent with the incorporation of about 4% of Mn into the ZnSe lattice.

The optical quality of a 1000 nm thick (Zn,Mn)Se epilayer with 2% Mn is examined by photoluminescence and reflectivity measurements in a magneto-optical cryostat at 1.6 K. Fig. 4 shows σ^+ - polarized luminescence spectra of the structure for magnetic fields of 0 to 7 T. Due to the large Zeeman splitting of the carriers, σ^- - polarized luminescence is completely suppressed already at a very small field of about 0.3 T. At $B=0$, the luminescence spectrum is dominated by a donor-bound exciton line. With applied magnetic field, the giant Zeeman splitting results in a suppression of the bound exciton and thus in a gain of intensity of the free exciton line. The energy position of the free exciton is depicted by crosses in the inset of Fig. 4. The open and closed circles in this figure represent reflectivity data, detected for σ^+ - and σ^- - polarized light, respectively. The Mn concentration of the epilayer can be deduced by again fitting of the experimental value of the Zeeman splitting with a modified Brillouin function[12]. The result of the fitting procedure is indicated by lines in the inset of Fig. 4. The obtained value of 3% for the Mn concentration is in good agreement with the growth parameters and the magnetization measurements and indicates a good incorporation of the Mn into the host material.

In conclusion we have demonstrated the high quality growth of paramagnetic (Zn,Mn)Se epilayers on a Si(100) surface. The growth technique and surface preparation procedure are optimized by using As passivation and a sophisticated low temperature growth start. Magneto-optical and magnetic characterization demonstrate that the quality of epilayers is suitable for spin injection experiments.

The authors would like to thank K. Brunner for useful discussions and D. Supp for SEM measurements, as well as the DFG (SFB 410), Darpa, and the German BMBF for financial support.

-
- [1] G. Schmidt, L. W. Molenkamp, A. T. Filip, and B. J. van Wees, Phys. Rev. B **62**, R4790 (2000).
 - [2] R. Fiederling, G. Reuscher, W. Ossau, G. Schmidt, A. Waag, and L. W. Molenkamp, Nature (London) **402**, 787 (2000).
 - [3] G. Schmidt, G. Richter, P. Grabs, D. Ferrand, and L.W. Molenkamp, Phys. Rev. Lett. **87**, 22703 (2001).
 - [4] Jantsch W, Wilamowski Z, Sandersfeld N, Muhlberger M, Schaffler F, Physica E **13**, 504 (2002)
 - [5] R. D. Bringans, D. K. Biegelsen, L. E. Swartz, F. A. Ponce, J. C. Tramontana, Phys. Rev. B **45**, 13400 (1992)
 - [6] C. Chauvet, C. Guénaud, P. Vennéguès, E. Tournié, J.P. Faurie, Journal of Crystal Growth **201**, 514 (1999).
 - [7] A. Ishizaka, Y. Shiraki, J. Electrochem. Soc. **133**, 667 (1986).
 - [8] D. J. Eaglesham, G. S. Higashi, and M. Cerullo, Appl. Phys. Lett. **59**, 685 (1991).
 - [9] L. Kipp, D.K. Biegelsen, J.E. Northrup, L.E. Swartz, and R.D. Bringans, Phys. Rev. Lett. **76**, 2810 (1996)
 - [10] J. A. Gaj, R. Planel, G. Fishman, Solid State Commun. **29**, 435(1979).
 - [11] W. Y. Yu, A. Twardowski, L. P. Fu, A. Petrou, B. T. Jonker, Phys. Rev. B **51**, 9722 (1995).
 - [12] For details see: D. Keller, D. R. Yakovlev, B. König, W. Ossau, Th. Gruber, A. Waag, L. W. Molenkamp, and A. V. Scherbakov, Phys. Rev. B **65**, 035313 (2002).